Electronic Supplementary Material

Ratiometric fluorescence immunoassay of SARS-CoV-2 nucleocapsid protein via Si-FITC nanoprobe-based inner filter effect

Guobin Mao[1,§], Yang Yang[3,§], Shijie Cao[1,2,§], Silu Ye[1], Yifang Li[1], Wei Zhao[1], Hongwei An[2], Yingxia Liu[3] (✉), Junbiao Dai[1], and Yingxin Ma[1] (✉)

[1] *CAS Key Laboratory of Quantitative Engineering Biology, Guangdong Provincial Key Laboratory of Synthetic Genomics and Shenzhen Key Laboratory of Synthetic Genomics, Shenzhen Institute of Synthetic Biology, Shenzhen Institutes of Advanced Technology, Chinese Academy of Sciences, Shenzhen 518055, China*

[2] *Guangxi University of Chinese Medicine, Nanning 530001, China*

[3] *Shenzhen Key Laboratory of Pathogen and Immunity, National Clinical Research Center for infectious disease, State Key Discipline of Infectious Disease, Shenzhen Third People's Hospital, Second Hospital Affiliated to Southern University of Science and Technology, Shenzhen 518112, China*

[§] *Guobin Mao, Yang Yang, and Shijie Cao contributed equally to this work.*

Supporting information to https://doi.org/10.1007/s12274-022-4740-5

Address correspondence to Yingxia Liu, yingxialiu@hotmail.com; Yingxin Ma, yx.ma1@siat.ac.cn

TSINGHUA UNIVERSITY PRESS Springer

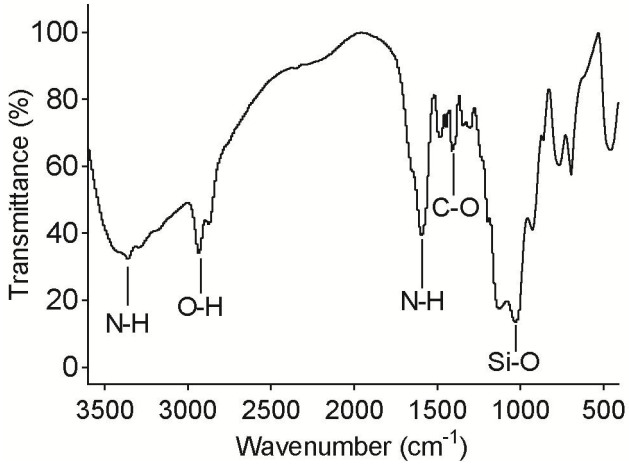

Figure S1 FTIR spectrum of Si-FITC NPs.

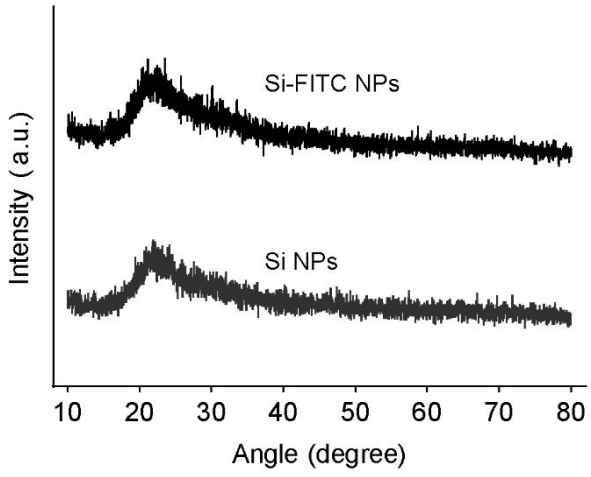

Figure S2 XRD spectra of Si-FITC NPs and Si NPs.

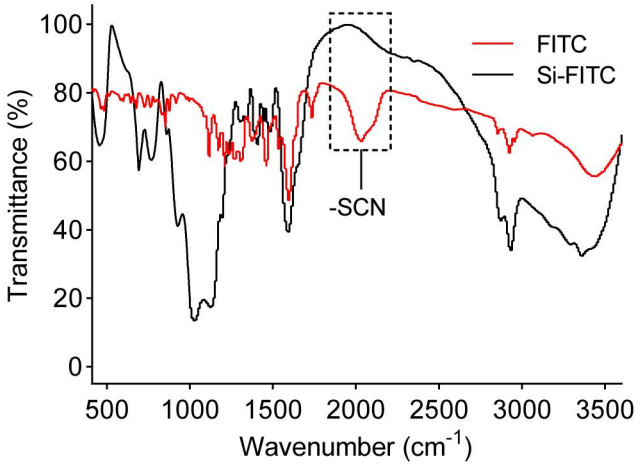

Figure S3 FTIR spectrum of FITC and Si-FITC NPs.

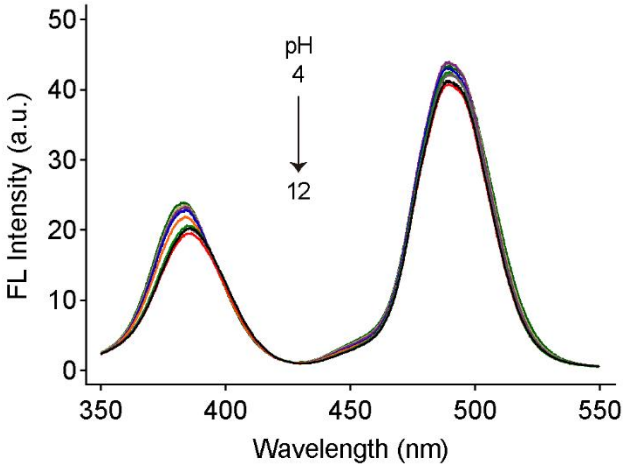

Figure S4 Synchronous fluorescence spectra of Si-FITC NPs in Tris buffer with different pH.

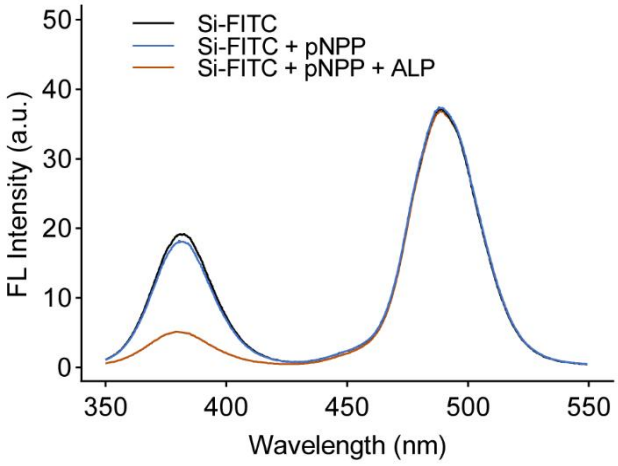

Figure S5 Synchronous fluorescence spectrum of Si FITC NPs, Si FITC NPs + pNPP, and Si FITC NPs + pNPP + ALP.

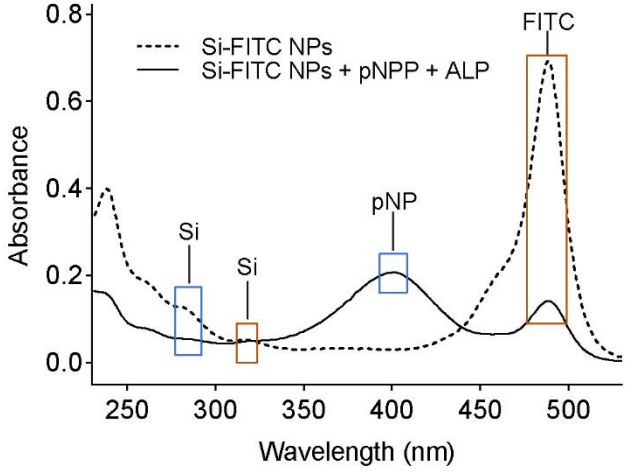

Figure S6 UV-vis absorption spectra of Si-FITC NPs in the absence or present of ALP + pNPP.

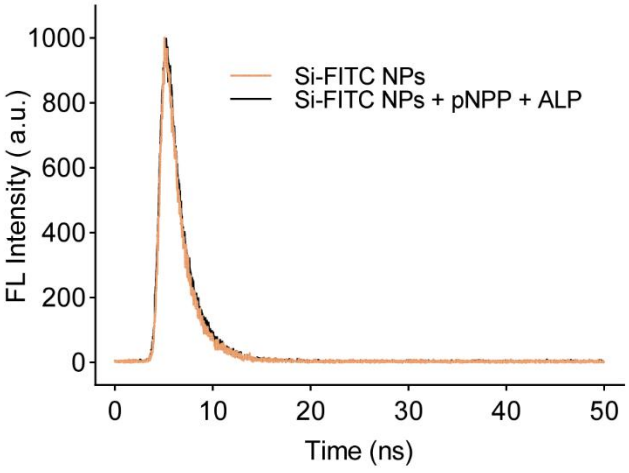

Figure S7 Fluorescence lifetime decay curves of Si-FITC NPs in the absence or present of pNPP and ALP.

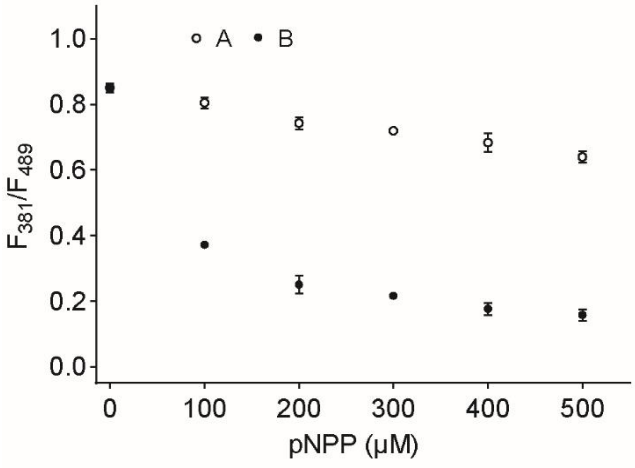

Figure S8 Fluorescence intensity ratio of Si-FITC NPs upon the addition of different concentrations of pNPP and 20 U/L ALP. A. Si-FITC NPs + pNPP, B. Si-FITC NPs + pNPP +ALP.

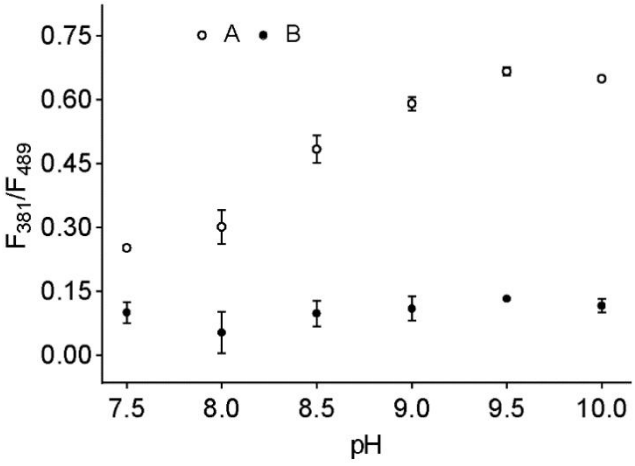

Figure S9 Fluorescence intensity ratio response of Si-FITC NPs/pNPP system to ALP under different pH. A. Si-FITC NPs + pNPP, B. Si-FITC NPs + pNPP + ALP.

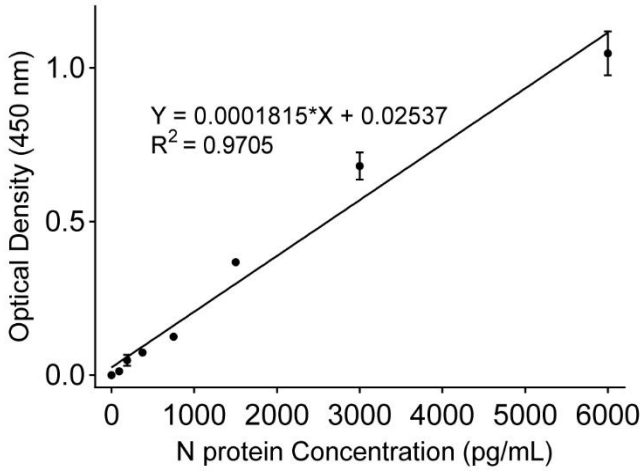

Figure S10 Detection of N protein using commercial ELISA Kit.

Table S1 Surface element composition of Si-FITC NPs and Si dots

Sample functional groups	BE (eV)	Percentages (%)			
		Si-FITC NPs		Si dots	
		N 1s	O 1s	N 1s	O 1s
C-N=C	399.17	77.74		82.52	
C-N	401.06	22.26		17.48	
C=O / Na-OH	531		37.1		60.48
C-O / Si-O	532.22		62.9		39.52

Table S2 Comparison of the this work with other reported methods for the detection of ALP.

Sensing System	Method	Linear Range (U/L)	LOD (U/L)	References
Fluorescent polydopamine nanoparticles	Fluorometry	1 - 80	0.34	[1]
Eu $(DPA)_3$@Lap-Cu^{2+}	Fluorometry	0.5 - 60	0.5	[2]
Calcein-Ce^{3+}	Fluorometry	0.1 - 0.4, 0.4 - 1.2	0.023	[3]
AA2P-OPD System	Fluorometry	0.1 - 30	0.06	[4]
TPEPy-Py	Fluorometry	1 - 1000	6.6	[5]
N-doped carbon quantum dots	Electrochemistry	5 - 360	1.1	[6]
Cu_xO nanopyramid islands	Electrochemistry	0.5 - 40	0.33	[7]
DEA-AP	Colorimetry	0.01 - 10	0.01	[8]
DNA-Cu (II) complexes	Colorimetry	20 - 200	0.84	[9]
Si-FITC NPs	Fluorometry	0.5 - 20	0.08	**This work**

Table S3 Comparison between other reports and this work on SARS-CoV-2 N protein detection.

Diagnosis type	Sensing System	Method	Linear Range (ng/ml)	LOD (ng/ml)	References
Antigen	AuNPs	Colorimetric	150 - 650	150	[10]
Antigen	Carbon black nanomaterial	Electrochemistry	10 - 600	8	[11]
Antigen	MagPlex	Electrochemistry	-	0.05	[12]
Antigen	Cotton-tipped electrode	Electrochemistry	1 - 1000	0.0008	[13]
Antigen	Automated microfluidic chemiluminescent ELISA device	Electrochemistry	0.062 - 1000	0.06	[14]
Antigen	AuNPs	Electrochemistry	0.001 - 100	0.0004	[15]
Antigen	Au@PtNPs	Colorimetry	0.05 - 1.26	0.026	[16]
Antigen	UCNPs@mSiO$_2$	Fluorometry	2 - 200	2.2	[17]
Antigen	Latex Bead Conjugation	Fluorometry	-	0.65	[18]
Antibody	Single-domain antibodies	Electrochemistry	-	0.05	[19]
Antibody	Electrochemical capillary-flow device	Electrochemistry	0 - 100	5	[20]
Antibody	Nanostructured plasmonic gold	Fluorometry	-	1.6	[21]
Antibody	Au nanospikes	Electrochemistry	1.6 - 13500	0.08	[22]
Antibody	Gold nanocluster	Fluorometry	0.01 - 1000	0.038	[23]
Antigen	Si-FITC NPs	Fluorometry	0.01 - 10, 50 - 300	0.002	**This work**

Table S4 Determination results of SARS-CoV-2 N protein in human serum

Added (ng/ml)	Measured (ng/ml)	Recovery (%)	RSD (%)
10.00	9.52	95.17	13.01
100.00	107.41	107.41	5.44

Table S5 The raw qPCR data of the patients tested in Fig. 5. N represents 'not detected'

Specimen number	qPCR	Fluorescence intensity ratio change	qPCR/Sensing system diagnosis COVID-19 result
1	23.00	0.20	+/+
2	23.84	0.22	+/+
3	25.84	0.11	+/+
4	23.30	0.13	+/+
5	21.86	0.29	+/+
6	25.68	0.16	+/+
7	22.13	0.23	+/+
8	22.00	0.22	+/+
9	24.60	0.14	+/+
10	N	0.034	-/-
11	N	0.03	-/-
12	N	0.03	-/-
13	N	0.04	-/-
14	N	0.04	-/-

References

[1] Xiao, T.; Sun, J.; Zhao, J.; Wang, S.; Liu, G.; Yang, X. Fret effect between fluorescent polydopamine nanoparticles and MnO_2 nanosheets and its application for sensitive sensing of alkaline phosphatase. *ACS Appl Mater Interfaces* **2018,** *10*, 6560-6569.

[2] Zhao, J.; Wang, S.; Lu, S.; Sun, J.; Yang, X. A luminescent europium-dipicolinic acid nanohybrid for the rapid and selective sensing of pyrophosphate and alkaline phosphatase activity. *Nanoscale* **2018,** *10*, 7163-7170.

[3] Chen, C.; Zhao, J.; Lu, Y.; Sun, J.; Yang, X. Fluorescence immunoassay based on the phosphate-triggered fluorescence turn-on detection of alkaline phosphatase. *Anal Chem* **2018,** *90*, 3505-3511.

[4] Zhao, D.; Li, J.; Peng, C.; Zhu, S.; Sun, J.; Yang, X. Fluorescence immunoassay based on the alkaline phosphatase triggered in situ fluorogenic reaction of o-phenylenediamine and ascorbic acid. *Anal Chem* **2019,** *91*, 2978-2984.

[5] Zhang, X.; Ren, C.; Hu, F.; Gao, Y.; Wang, Z.; Li, H.; Liu, J.; Liu, B.; Yang, C. Detection of bacterial alkaline phosphatase activity by enzymatic in situ self-assembly of the aiegen-peptide conjugate. *Anal Chem* **2020,** *92*, 5185-5190.

[6] Niu, F.; Ying, Y.-L.; Hua, X.; Niu, Y.; Xu, Y.; Long, Y.-T. Electrochemically generated green-fluorescent N-doped carbon quantum dots for facile monitoring alkaline phosphatase activity based on the Fe^{3+}-mediating on-off-on-off fluorescence principle. *Carbon* **2018,** *127*, 340-348.

[7] Zhang, N.; Ruan, Y. F.; Zhang, L. B.; Zhao, W. W.; Xu, J. J.; Chen, H. Y. Nanochannels photoelectrochemical biosensor. *Anal Chem* **2018,** *90*, 2341-2347.

[8] Sun, J.; Zhao, J.; Bao, X.; Wang, Q.; Yang, X. Alkaline phosphatase assay based on the chromogenic interaction of diethanolamine with 4-aminophenol. *Anal Chem* **2018,** *90*, 6339-6345.

[9] Yang, J.; Zheng, L.; Wang, Y.; Li, W.; Zhang, J.; Gu, J.; Fu, Y. Guanine-rich DNA-based peroxidase mimetics for colorimetric assays of alkaline phosphatase. *Biosens Bioelectron* **2016,** *77*, 549-56.

[10] Behrouzi, K.; Lin, L. Gold nanoparticle based plasmonic sensing for the detection of SARS-CoV-2 nucleocapsid proteins. *Biosens Bioelectron* **2022,** *195*, 113669.

[11] Fabiani, L.; Saroglia, M.; Galata, G.; De Santis, R.; Fillo, S.; Luca, V.; Faggioni, G.; D'Amore, N.; Regalbuto, E.; Salvatori, P. et al. Magnetic beads combined with carbon black-based screen-printed electrodes for COVID-19: A reliable and miniaturized electrochemical immunosensor for sars-cov-2 detection in saliva. *Biosens Bioelectron* **2021,** *171*, 112686.

[12] Anderson, G. P.; Liu, J. L.; Esparza, T. J.; Voelker, B. T.; Hofmann, E. R.; Goldman, E. R. Single-domain antibodies for the detection of SARS-CoV-2 nucleocapsid protein. *Anal Chem* **2021,** *93*, 7283-7291.

[13] Eissa, S.; Zourob, M. Development of a low-cost cotton-tipped electrochemical immunosensor for the detection of SARS-CoV-2. *Anal Chem* **2021,** *93*, 1826-1833.

[14] Tan, X.; Krel, M.; Dolgov, E.; Park, S.; Li, X.; Wu, W.; Sun, Y. L.; Zhang, J.; Khaing Oo, M. K.; Perlin, D. S. et al. Rapid and quantitative detection of SARS-CoV-2 specific IgG for convalescent serum evaluation. *Biosens Bioelectron* **2020,** *169*, 112572.

[15] Eissa, S.; Alhadrami, H. A.; Al-Mozaini, M.; Hassan, A. M.; Zourob, M. Voltammetric-based immunosensor for the detection of SARS-CoV-2 nucleocapsid antigen. *Mikrochim Acta* **2021,** *188*, 199.

[16] Liang, C.; Liu, B.; Li, J.; Lu, J.; Zhang, E.; Deng, Q.; Zhang, L.; Chen, R.; Fu, Y.; Li, C. et al. A nanoenzyme linked immunochromatographic sensor for rapid and quantitative detection of SARS-CoV-2 nucleocapsid protein in human blood. *Sens Actuators B Chem* **2021,** *349*, 130718.

[17] Guo, J.; Chen, S.; Tian, S.; Liu, K.; Ni, J.; Zhao, M.; Kang, Y.; Ma, X.; Guo, J. 5G-enabled ultra-sensitive fluorescence sensor for proactive prognosis of COVID-19. *Biosens Bioelectron* **2021,** *181*, 113160.

[18] Grant, B. D.; Anderson, C. E.; Williford, J. R.; Alonzo, L. F.; Glukhova, V. A.; Boyle, D. S.; Weigl, B. H.; Nichols, K. P. SARS-CoV-2 coronavirus nucleocapsid antigen-detecting half-strip lateral flow assay toward the development of point of care tests using commercially available reagents. *Anal Chem* **2020,** *92*, 11305-11309.

[19] Anderson, G. P.; Liu, J. L.; Esparza, T. J.; Voelker, B. T.; Hofmann, E. R.; Goldman, E. R. Single-domain antibodies for the detection of SARS-CoV-2 nucleocapsid protein. *Anal Chem* 2021, 93, 7283-7291.

[20] Samper, I. C.; Sanchez-Cano, A.; Khamcharoen, W.; Jang, I.; Siangproh, W.; Baldrich, E.; Geiss, B. J.; Dandy, D. S.; Henry, C. S. Electrochemical capillary-flow immunoassay for detecting anti- SARS-CoV-2 nucleocapsid protein antibodies at the point of care. *ACS Sens* 2021, 6, 4067-4075.

[21] Liu, T.; Hsiung, J.; Zhao, S.; Kost, J.; Sreedhar, D.; Hanson, C. V.; Olson, K.; Keare, D.; Chang, S. T.; Bliden, K. P. et al. Quantification of antibody avidities and accurate detection of SARS-CoV-2 antibodies in serum and saliva on plasmonic substrates. Nat Biomed Eng 2020, 4, 1188-1196.

[22] Funari, R.; Chu, K. Y.; Shen, A. Q. Detection of antibodies against SARS-CoV-2 spike protein by gold nanospikes in an opto-microfluidic chip. *Biosens Bioelectron* 2020, 169, 112578.

[23] Oh, H. K.; Kim, K.; Park, J.; Im, H.; Maher, S.; Kim, M. G. Plasmon color-preserved gold nanoparticle clusters for high sensitivity detection of SARS-CoV-2 based on lateral flow immunoassay. *Biosens Bioelectron* 2022, 205, 114094.